7852 J. Med. Chem. 2010, 53, 7852–7863
DOI: 10.1021/jm101015z

Journal of Medicinal Chemistry Article

Design, Synthesis, Crystal Structures, and Antimicrobial Activity of Sulfonamide Boronic Acids as β-Lactamase Inhibitors†

Oliv Eidam,[‡,⊥] Chiara Romagnoli,[‡,§,⊥] Emilia Caselli,[§] Kerim Babaoglu,[‡,#] Denise Teotico Pohlhaus,[‡,∞] Joel Karpiak,[‡] Richard Bonnet,[∥] Brian K. Shoichet,*[,‡] and Fabio Prati*[,§]

[‡]*Department of Pharmaceutical Chemistry, Byers Hall, University of California San Francisco, 1700 4th Street, San Francisco, California 94158, United States,* [§]*Dipartimento di Chimica, Università degli Studi di Modena e Reggio Emilia, Via Campi 183, 41100 Modena, Italy, and* [∥]*Laboratoire de Bactériologie-Mycologie-Parasitologie 58, Centre de Biologie, Centre Hospitalier Universitaire, Boulevard Montalembert, 63003, Clermont-Ferrand Cedex 1, France.* [⊥]*Both authors contributed equally to this work.* [#]*Current address: Gilead, Foster City, California, United States.* [∞]*Current address: GlaxoSmithKline, Raleigh, North Carolina, United States.*

Received August 4, 2010

We investigated a series of sulfonamide boronic acids that resulted from the merging of two unrelated AmpC β-lactamase inhibitor series. The new boronic acids differed in the replacement of the canonical carboxamide, found in all penicillin and cephalosporin antibiotics, with a sulfonamide. Surprisingly, these sulfonamides had a highly distinct structure−activity relationship from the previously explored carboxamides, high ligand efficiencies (up to 0.91), and K_i values down to 25 nM and up to 23 times better for smaller analogues. Conversely, K_i values were 10−20 times worse for larger molecules than in the carboxamide congener series. X-ray crystal structures (1.6−1.8 Å) of AmpC with three of the new sulfonamides suggest that this altered structure−activity relationship results from the different geometry and polarity of the sulfonamide versus the carboxamide. The most potent inhibitor reversed β-lactamase-mediated resistance to third generation cephalosporins, lowering their minimum inhibitory concentrations up to 32-fold in cell culture.

Introduction

The expression of β-lactamases is the most common cause of resistance to β-lactam antibiotics, such as penicillins and cephalosporins.[1−3] β-Lactamases catalyze the hydrolysis of the critical β-lactam ring in β-lactam antibiotics, thereby inactivating them.[4] To overcome this problem, β-lactamase inhibitors, such as clavulanic acid or sulbactam, are coadministered with the primary β-lactam (Figure 1).[5,6] However, the active core of these inhibitors remains a β-lactam ring, enabling the rapid development of resistance.[7] For example, AmpC, a class C β-lactamase expressed by many nosocomial pathogens, is not inhibited by clavulanic acid or sulbactam at clinically relevant concentrations, leading to substantial problems in the clinic.[8,9]

The broad activity of class C β-lactamases has motivated a search for novel inhibitors. New departures based on the β-lactam core have shown substantial, typically mechanism-based activity in vitro and in vivo as inhibitors.[10−13] There is also a motivation to discover inhibitors structurally unrelated to β-lactams, which might evade pre-evolved bacterial resistance mechanisms.[14−16] Lacking the β-lactam core, these inhibitors should not be hydrolyzed by mutant enzymes that arise in response to new β-lactams, should not be recognized by β-lactam signaling receptors, and might be unaffected by porin channel mutations that decrease permeability.[2,17]

Boronic acids are transition-state analogues that lack the β-lactam recognition motif and are distinct enough chemically to evade pre-evolved resistance mechanisms.[17−19] They form dative, rapidly reversible covalent bonds with the active site serine, forming a tetrahedral adduct that mimics the high-energy intermediate of β-lactams along the β-lactamase reaction coordinate (Figure 2).[20]

We found previously that acylglycyl boronic acids bearing side chains characteristic of penicillins and cephalosporins (R_1 group in Figure 2A) have K_i values as low as 20 nM against AmpC.[19] Using a structure-based drug design approach, we designed *m*-carboxyphenylboronic acids having a negatively charged group in a position corresponding to the C4 of cephalosporins, such as cephalothin (Figure 1).[21,22] Compound **18c** has a K_i value of 1 nM, improving potency up to 300-fold compared to the corresponding acylglycylboronic acid **10c** (Table 1).

In the crystal structure of the AmpC/**18c** complex, the oxygen atom of the carboxamide forms a hydrogen bond with Asn152, a conserved residue in the AmpC active site, while the carboxamide nitrogen hydrogen-bonds with the backbone carbonyl of Ala318, a residue that contributes to the enzyme's oxyanion hole (Figure 3A). In an unrelated series of noncovalent β-lactamase inhibitors, discovered by molecular docking, a sulfonamide group is similarly positioned and makes the same interactions (Figure 3B).[23]

It therefore seemed interesting to replace the ubiquitous carboxamide, present in the R_1 side chain of both β-lactams and their boronic acid mimics, by a sulfonamide (Scheme 1). Whereas sulfonamide replacements for carboxamides date

†The coordinates and structure factors have been deposited in the Protein Data Bank with the accession codes 3O86, 3O87, and 3O88 for AmpC in complex with **4**, **9**, and **17**, respectively.

*To whom correspondence should be addressed. For B.K.S.: phone, 415-514-4126; fax, 415-514-4260; e-mail, shoichet@cgl.ucsf.edu. For F.P.: phone, +39-059-2055056; fax, +39-059-373543; e-mail, fabio.prati@unimore.it.

 Published on Web 10/14/2010

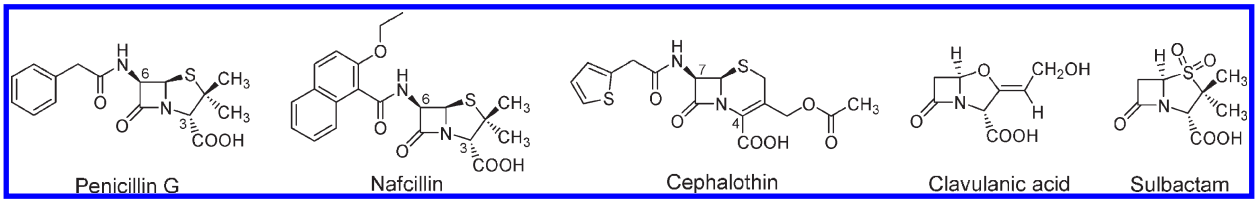

Figure 1. Penicillin and cephalosporin antibiotics and two clinically used β-lactamase inhibitors.

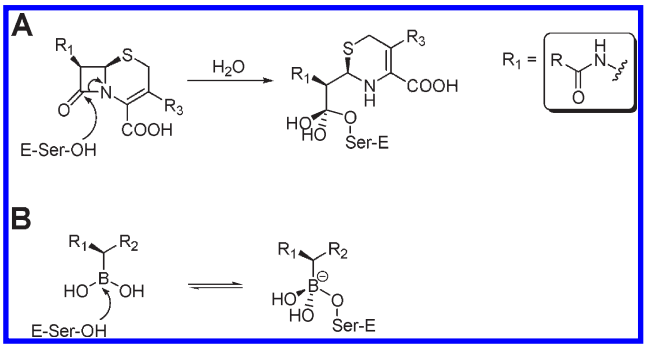

Figure 2. Boronic acids as transition-state analogues: (A) hydrolytic attack on the β-lactam ring of a cephalosporin and formation of the high-energy intermediate; (B) binding of β-lactamase to a boronic acid and formation of a transition-state analogue.

back to the seminal synthetic work of Sheehan in the 1950s,[24] these derivatives were never used clinically and, as far as we know, have never been explored among β-lactamase inhibitors previous to this year. Very recent work by Tan et al. at Merck revealed two arylsulfonamide boronic acids with activity in the low micromolar range (IC_{50}[a] between 0.57 and 5.6 μM) against five different β-lactamases.[25]

We synthesized 10 sulfonamide boronic acids and tested their inhibition of AmpC β-lactamase. Among them are seven different R_1 groups including the penicillin G and nafcillin side chains. We found that the simplest of these new sulfonamides were unexpectedly the most potent (K_i values in the 25 nM range), over 23 times more than their carboxamide analogues, and that the SAR of this series differed completely from what was observed in the carboxamide series. To understand these differences, we determined X-ray structures of three inhibitors in complex with AmpC. Finally, we investigated the efficacy of the most potent inhibitors to reverse antibiotic resistance in bacterial cell cultures.

Results

Design. The geometry and electronic properties of a sulfonamide are quite different from those of a carboxamide, and we were interested in how this substitution would affect affinity (Scheme 1). First, we explored the sulfonamide substitution with a methyl alone as the R group. Since this compound was unexpectedly potent against AmpC, we then synthesized and tested sulfonamide boronic acids with seven more elaborate R groups (Table 1). Finally, we synthesized

Table 1. K_i Values (μM) of Sulfonamide and Carboxamide Boronic Acids[a]

Sulfonamide boronic acids			Carboxamide boronic acids		
ID	Structure	K_i (μM)	ID	Structure*	K_i (μM)
3		0.789	**3c**	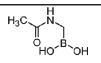	18.5
4	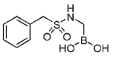	0.070	**4c**	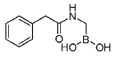	0.570
5	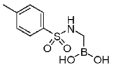	0.210			
6	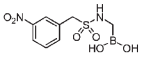	0.189			
7	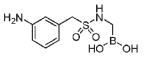	0.106			
8	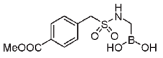	0.120			
9	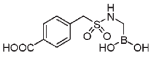	0.025			
10	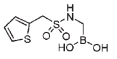	N.A.[#]	**10c**	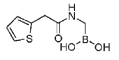	0.320
11	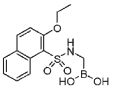	0.670	**11c**	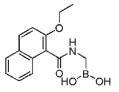	0.033
16	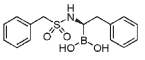	3.723			
17	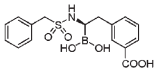	0.430	**17c**[‡]	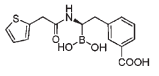	0.039
18	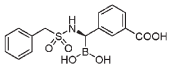	N.A.[#]	**18c**[‡]	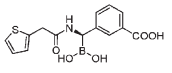	0.001

[a] (*) Compounds **3c**–**11c** have been published in ref 19 and 18c in ref 21. Compound 17c has been synthesized and tested in this study. (#) Not applicable: compound not obtained. (‡) Compounds 17c and 18c have a thiophene in the R_1 side chain and are therefore not exact analogues of 17 and 18, respectively.

molecules with a benzyl and *m*-carboxybenzyl groups as R_2 substituents.

Synthesis. The sulfonamidomethaneboronic acids **3**–**9** and **11** were synthesized through sulfonylation of the aminomethaneboronate **2** (Scheme 2). The key intermediate **2** was obtained by treating the chloromethylboronic acid pinacol ester **1** with lithium bis(trimethylsilyl)amide.[19] In situ deprotection of **2** with equimolar methanol, followed by condensation with suitable sulfonyl chlorides, afforded the sulfonamidomethaneboronic acids **3**–**9** and **11**.

Compound **10** (Table 1), bearing the cephalothin side chain, could not be obtained because of instability of the

[a] Abbreviations: LE, ligand efficiency (=($\Delta G_{binding}$ (kcal/mol))/(number of non-hydrogen atoms)); PDB, Protein Data Bank; IC_{50}, half-maximal inhibitory concentration; SAR, structure–activity relationship; MIC, minimum inhibitory concentration; CLSI, Clinical and Laboratory Standards Institute; CAZ, ceftazidime; FOX, cefoxitin; THF, tetrahydrofuran; TLC, thin layer chromatography.

suitable sulfonyl chloride. In fact, several attempts to obtain the (thiophene-2-yl)methanesulfonylchloride led to the corresponding 2-chloromethylthiophene instead, as reported for other electron rich phenylmethanesulfonyl chlorides.[26]

According to recent literature reports, related sulfonylaminomethaneboronate compounds[27,28] can also be prepared by alkylation of suitable *N*-*tert*-butylsulfonamides with pinacol chloromethaneboronate **1**, followed by acidic *tert*-butyl removal. However, this reaction sequence proved to be less efficient, and the method was therefore abandoned.

Following our previous approach with carboxamides,[21] we attempted to synthesize compound **18** (Table 1), but the synthesis failed because protodeboronation during sulfonylation reaction occurred. The loss of the boronic moiety may occur because of stabilization of the intermediate carbanion formed when a base coordinates to boron.[29] Because the presence of the *m*-carboxyphenyl ring in the present case can account for this stabilization, we decided to add an extra carbon between the boron atom and the phenyl ring (Scheme 3). Therefore, to build the more elaborated inhibitors **16** and **17**, boronates **12a**,**b** were first homologated with chloromethyllithium.[30] Subsequent Matteson stereoselective homologation with dichloromethyllithium,[29,31−33] followed by substitution with bis(trimethylsilyl)amide and sulfonylation afforded compounds **15a**,**b**. The use of (+)-pinanediol as chiral auxiliary allowed the formation of the final *R* configuration, which mimics the stereochemistry of carbon atom C6/7 of penicillin/cephalosporin. The conversion of pinanediol esters **15a**,**b** to free boronic acids **16** and **17** was achieved through transesterification with phenylboronic acid in a biphasic acetonitrile/water system.[34]

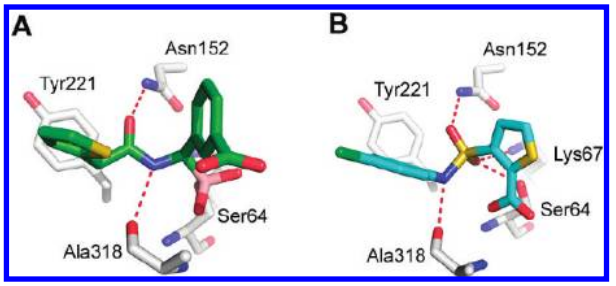

Figure 3. Inspiration for sulfonamide boronic acids. (A) The carboxamide of boronic acid **18c** hydrogen-bonds with Asn152 and Ala318 of AmpC β-lactamase (PDB code 1MXO). Carbon atoms of inhibitor are colored green, oxygens red, nitrogens blue, sulfur yellow, boron atom amaranth pink. (B) The sulfonamide of a noncovalent β-lactamase inhibitor hydrogen-bonds with Asn152, Ala318, Ser64, and Lys67 (PDB code 1L2S). Carbon atoms of inhibitor are colored cyan, oxygens red, nitrogens blue, sulfur yellow, chloride green.

Scheme 1. Conversion of Carboxamide Boronic Acids into Sulfonamide Boronic Acids

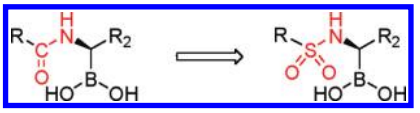

Enzymology and Binding Affinities. Except for those binding in the low nanomolar range, all previously studied boronic acids inhibitors of AmpC β-lactamase have been reversible, competitive inhibitors with fast-on, fast-off rates.[17,18] The same was found for the new sulfonamide boronic acid series, as no incubation effect was detected for any of the compounds.

To investigate the effect of the carboxamide replacement with a sulfonamide, we first measured the potency of methanesulfonamide boronic acid **3** (Table 1). Compound **3** inhibits AmpC with a K_i of 789 nM, a 23-fold improvement of potency compared to the carboxamide analogue **3c** (K_i = 18.5 μM). The high affinity of this relatively small molecule prompted us to study larger derivatives. Compound **4**, bearing the penicillin G side chain has a K_i of 70 nM, a 10-fold improvement over the initial sulfonamide **3** and an 8-fold improvement compared to its exact carboxamide analogue **4c** (K_i = 570 nM) (Table 1).[19] Because compound **5**, isomer of compound **4**, has a K_i of 210 nM, we decided to focus on benzylic derivatives and synthesized compounds **6**−**9**, for which required sulfonylchlorides were commercially available or the final products easily accessible. Although most of those derivatives have a lower potency than **4**, compound **9**

Scheme 2. General Scheme of the Synthesis of Sulfonamidomethaneboronic Acids

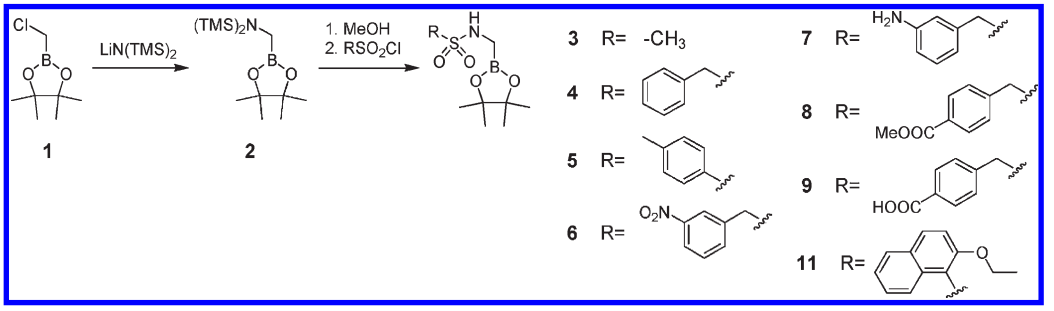

Scheme 3. Asymmetric Synthesis of 1-Sulfonamido-2-phenylethaneboronic Acids **16** and **17**

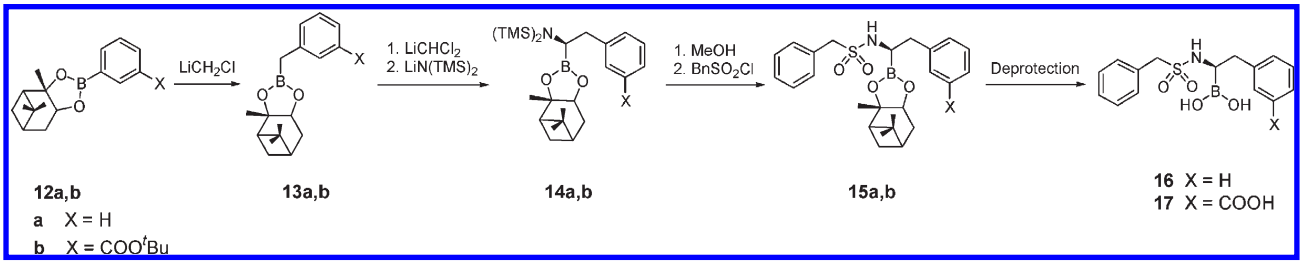

Table 2. Data Collection and Refinement Statistics

	AmpC/**4**	AmpC/**9**	AmpC/**17**
PDB code	3O86	3O87	3O88
	Data Collection		
space group	*C*2	*C*2	*C*2
cell dimension			
a, *b*, *c* (Å)	118.34, 76.88, 97.76	118.13, 76.19, 97.38	118.03, 77.39, 97.41
α, *β*, *γ* (deg)	90.00, 116.11, 90.00	90.00, 116.16, 90.00	90.00, 115.90, 90.00
resolution (Å)	30−1.60 (1.69−1.60)[a]	40−1.78 (1.88−1.78)[a]	30−1.64 (1.72 − 1.64)[a]
R_{merge} (%)	4.5 (44.0)[a]	5.8 (45.5)[a]	4.4 (44.8)[a]
completeness (%)	99.0 (98.6)[a]	97.5 (95.7)[a]	98.5 (99.5)[a]
$I/\sigma(I)$	16.4 (3.1)[a]	12.6 (2.7)[a]	15.3 (2.6)[a]
redundancy	3.85 (3.81)[a]	2.95 (2.95)[a]	3.05 (3.05)[a]
	Refinement		
resolution (Å)	29.58−1.60	38.43−1.78	29.54−1.64
no. reflections	102 732	72 662	95 179
R_{work}/R_{free} (%)	16.7/19.3	18.8/23.2	18.1/21.0
no. atoms			
protein[b]	5540	5448	5595
ligand[b]	30	36	50
water	819	519	744
B-factor (Å^2)			
protein[b]	20.97	22.31	24.59
ligand[b]	26.41	26.32	32.02
water	33.62	31.03	35.15
rms deviation			
bond length (Å)	0.010	0.011	0.011
bond angle (deg)	1.323	1.355	1.374

[a] Values in parentheses represent values for the highest resolution shells. [b] Calculated for both molecules in asymmetric unit.

has a K_i of 25 nM, a 3-fold improvement versus compound **4**. We tried to synthesize compound **10**, the exact analogue of the carboxamide **10c**, but found that the required (thiophene-2-yl)methanesulfonylchloride was unstable. Unexpectedly, compound **11**, bearing the nafcillin side chain, inhibits AmpC with a K_i of 670 nM, 20-fold weaker than the carboxamide analogue **11c** (K_i = 33 nM). This was another indicator that the SAR changes substantially in the sulfonamide series.

In the carboxamide series, addition of a *m*-carboxybenzyl group to **10c** had resulted in a 7-fold improvement of potency for compound **17c**. We decided to investigate the same modification for the sulfonamide **4** and synthesized the chiral compound **17**. This latter has a K_i of 430 nM; thus, rather than a 7-fold improvement, adding a *m*-carboxybenzyl to compound **4** led to a 6-fold decrease in inhibition. Compound **16**, only with a benzyl as R_2 group, has an even worse K_i of 3.7 μM. The weaker potency of compounds **16** and **17** further demonstrate the changed SAR resulting from the carboxamide to sulfonamide conversion.

Structural Analysis. To investigate the structural basis of the carboxamide to sulfonamide conversion, we determined cocrystal structures of AmpC in complex with **4**, **9**, and **17** (Table 2). All complexes were obtained from the same crystallization condition yielding centered monoclinic *C*2 crystals with two AmpC complexes in the asymmetric unit. The positions of the inhibitors in the active site were unambiguously identified in both chains in the initial $F_o - F_c$ difference density maps (Figure 4). With the exception of the complex with compound **4**, the conformations of the inhibitors were very similar in both monomers.

For all three inhibitors, electron density connected the Oγ of the catalytic Ser64 to the boron atoms of the inhibitors. The boron geometry was tetrahedral, as expected, and key hydrogen bond interactions in the active site closely resembled those typically observed in β-lactamase structures with transition-state analogues and with β-lactams (Figure 5A−C).[14,19,21,22] One oxygen atom of the boronic acid is placed in the "oxyanion hole" formed by the backbone amide groups of Ser64 and Ala318. The other oxygen atom of the boronic acid interacts with the conserved Tyr150, which contributes to activating the deacylating water Wat402 for attack on the acyl intermediate.[15,35−39] Both oxygen atoms are also within hydrogen bonding distance to the conserved water molecule Wat402.

The crystal structure of compound **4** (K_i = 70 nM) in complex with AmpC was determined at 1.60 Å (Figure 5A). Whereas there were several differences between the two monomers in the asymmetric unit, such as the rotation of the benzyl ring to stack with Tyr221 in either a parallel or herringbone conformation, we will focus on the interaction in chain A. Here, one oxygen atom of the sulfonamide hydrogen-bonds to Asn152 (nitrogen−oxygen distance: 2.6 Å). The other sulfonamide oxygen atom hydrogen-bonds with a water molecule bridging to Gln120. The benzyl group makes a T-shaped $\pi-\pi$ interaction (90° angle) with Tyr221. The sulfonamide nitrogen interacts neither with the protein nor with a well-ordered water molecule.

To understand the influence of the *p*-carboxylate group, responsible for a 3-fold increase affinity of compound **9** (K_i = 25 nM) compared to compound **4**, we determined the crystal structure of the AmpC/**9** complex to 1.78 Å resolution (Figure 5B). The conformation of **9** is similar in both monomers and resembles the conformation of **4** observed in chain A except that the plane of its phenyl ring is slightly offset relative to that of **4** (Figure 5D). The slightly altered conformation allows the *p*-carboxylate group to hydrogen-bond with the side chain hydroxyl and amide

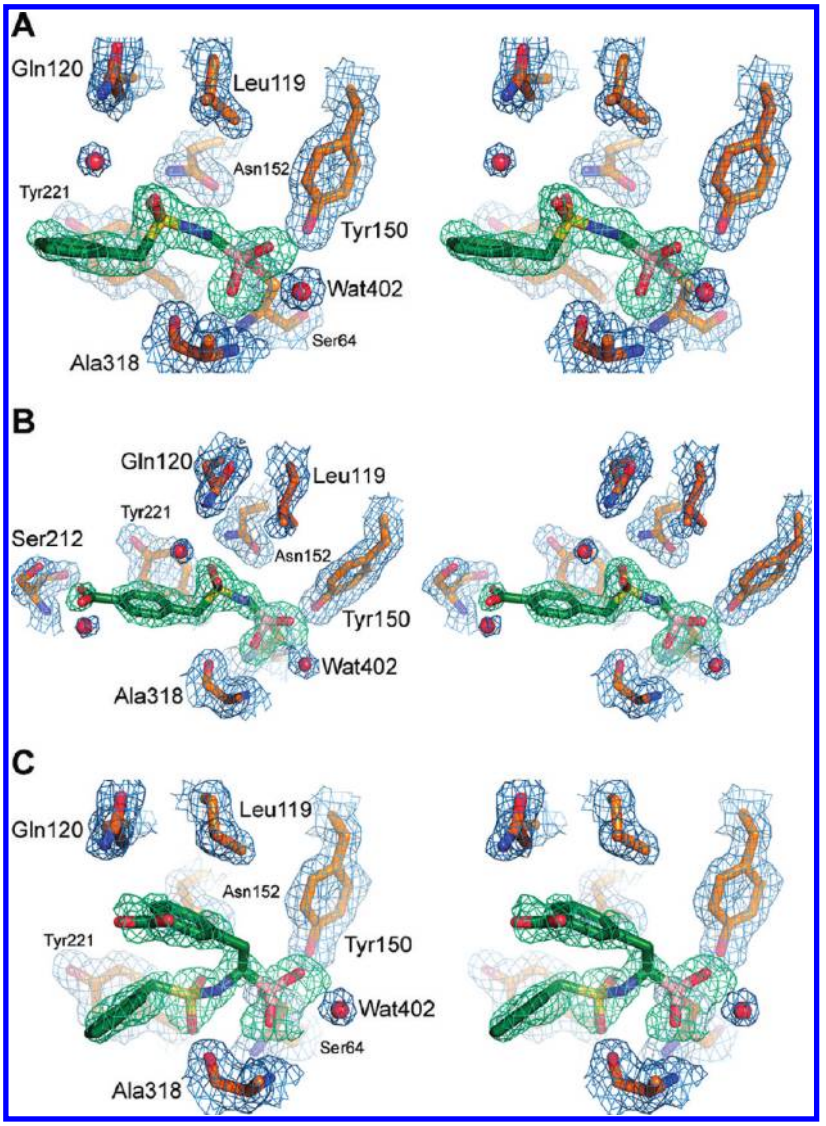

Figure 4. Stereoviews of initial $F_o - F_c$ electron densities (green, 2.5σ contour level) of sulfonamide boronic acids and final $2F_o - F_c$ densities (blue, 1σ contour level) of AmpC and conserved water molecules: (A) compound **4** in chain A; (B) compound **9**; (C) compound **17**. Inhibitor carbons are in green, enzyme carbons in gold, oxygens in red, nitrogens in blue, sulfurs in yellow, borons in amaranth pink.

nitrogen of Ser212. The other carboxylate oxygen atom hydrogen-bonds with an ordered water molecule.

To understand the reduced activity of **17** (K_i = 430 nM) against AmpC relative to compounds **4** and **9**, we determined its crystal structure in complex with AmpC at 1.64 Å resolution (Figure 5C). In this complex, the boron−carbon bond is rotated by 90° compared to the conformation adopted by compound **4**. This is necessary to accommodate the additional *m*-carboxybenzyl R_2 group of **17**. Consequently, the sulfonamide is reoriented in the active site, placing the benzylsulfonamide in a totally different location relative to compounds **4** and **9** (Figure 5E). One sulfonamide oxygen of compound **17** makes stretched hydrogen bonds with Asn152 and Lys67 (3.2 and 3.1 Å, respectively), and the nitrogen atom of the sulfonamide hydrogen-bonds with the backbone amide of Ala318 (3.1 Å), an interaction missed in the other two structures. Conversely, the second oxygen atom now abuts the backbone carbonyl of Ala318 (2.8 Å) and the quality of the other sulfonamide hydrogen bonds, as judged by distance and angle, has deteriorated substantially. The R phenyl group makes a T-shaped $\pi-\pi$ interaction with Tyr221 but in a different conformation than observed in the AmpC/**4** and AmpC/**9** complex structures.

Antimicrobial Activity. The antiresistance activity of inhibitors **4** and **9** was investigated against clinical bacteria exhibiting high level of resistance against third-generation cephalosporins, such as ceftazidime, via expression of class A or class C β-lactamases. When the compounds were administrated alone in a disk diffusion assay, they had little or no detectable activity on bacteria growth, as expected. However, in combination with ceftazidime the compounds produced a large inhibition halo surrounding the disk (Figure 6A). This inhibition of the bacterial growth revealed clear synergy between these compounds. The size of the inhibition zone was similar for both compounds and showed improved inhibition of bacterial growth compared to ceftazidime alone.

Antimicrobial activity was investigated quantitatively to determine the minimum inhibitory concentrations (MICs) of the β-lactam/inhibitor combination necessary to inhibit the bacterial growth (Table 3). The MICs of β-lactams alone against the strains corresponded to a high level of resistance according to Clinical and Laboratory Standards Institute

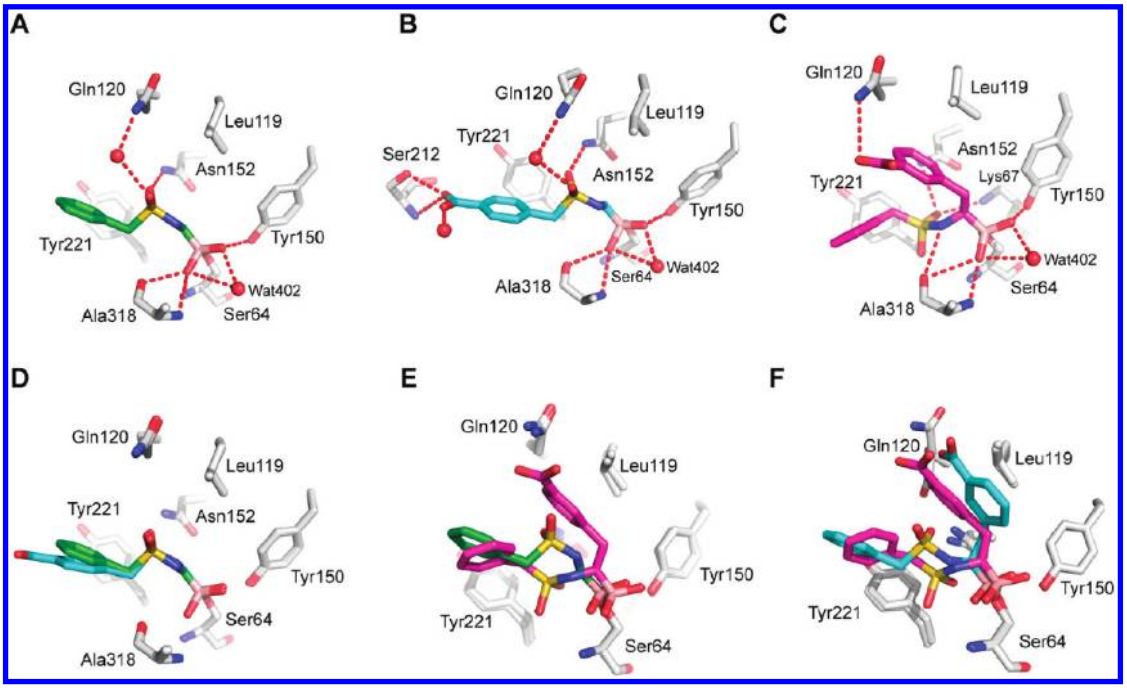

Figure 5. Polar interactions of sulfonamide boronic acids with AmpC and comparison of conformations. Enzyme residues are depicted in atom colors (gray carbons, red oxygens, blue nitrogens). Hydrogen bonds are shown as red dashes, water molecules as red spheres. (A) Compound **4** (green carbon atoms) in chain A. (B) Compound **9** (cyan carbon atoms). (C) Compound **17** (magenta carbon atoms). (D) Superposition of compound **9** on compound **4**. (E) Superposition of compound **17** on compound **4**. (F) Superposition of a model of **17** (cyan carbon atoms) on its actual crystal structure (magenta carbon atoms). See Discussion.

(CLSI) standards.[40] The compounds had no measurable antibiotic activity when used alone. In combination with β-lactams, the compounds decreased MIC values by 8-fold on average. Interestingly, even larger relative decreases in MIC values were observed for an *E. coli* strain producing the plasmid-mediated class A β-lactamase CTX-M-14 (16- to 32-fold). This offers preliminary evidence that the sulfonamide boronic acids may inhibit both class C β-lactamases and class A enzymes, consistent with studies revealing activity against this class of enzymes in the low micromolar range described in this study (Table 4 and below) and results from Tan and colleagues.[25] More detailed studies will be necessary before inhibition of the class A β-lactamases can be shown to be broad or robust.

A traditional β-lactam resistance mechanism is the up-regulation of β-lactamase-encoding gene transcription caused by β-lactams such as cefoxitin and the β-lactamase inhibitor clavulanate. To test the role of compounds on the induction of AmpC expression, we investigated their ability to potentiate the action of the β-lactam ceftazidime. We compared the potentiation effect of compounds with that of cefoxitin (Figure 6B and Figure 6C). Agar plates were inoculated with *K. pneumoniae* and *E. cloacae* strains in which AmpC expression is inducible. A ceftazidime-containing disk and a disk containing the inhibitors (cefoxitin or compounds **4** and **9**) were placed on each plate. As ceftazidime diffuses from disks into the agar, a clear zone is created around the ceftazidime-containing disk, indicating where bacteria are unable to grow. The shape of this halo in the vicinity of the inhibitor-containing disk indicated the effect of these compounds on the induction of AmpC. The inhibition halos normally surrounding ceftazidime were substantially diminished in the regions nearest the cefoxitin disk. This well-known antagonist picture is characteristic of the *ampC* gene induction by cefoxitin. The antagonist picture was replaced by a synergic picture with compounds **4** and **9**; the inhibition halos of ceftazidime were dramatically increased in the region near the compound disks. This result indicates that the compounds inhibit AmpC and do not induce significant up-regulation of AmpC-encoding genes, in contrast to β-lactams such as cefoxitin.

Selectivity. To investigate the selectivity of sulfonamide boronic acids, compounds **4** and **9** were tested against the serine protease α-chymotrypsin, the cysteine protease cruzain, and the class A β-lactamase CTX-M-9, which is structurally different from AmpC (Table 4). Compounds **4** and **9** showed no measurable inhibition at 100 μM against cruzain and α-chymotrypsin. Interestingly, the compounds are active against CTX-M-9 with IC_{50} values in the low micromolar range. The K_i values corresponding to the IC_{50} values are 2.529 and 0.552 μM, respectively, indicating 36-fold and 22-fold selectivity toward AmpC versus CTX-M-9 β-lactamase.

Discussion

Three key observations emerge from this study. First, the new sulfonamide boronic acids derived from the conversion of the canonical R_1 carboxamide retain substantial inhibition activity against β-lactamases. Second, they rescue antibiotic resistance when used in combination with third generation antibiotics in bacterial cell cultures. Third, this superficially modest substitution changes the geometry of the inhibitors enough to scramble the SAR observed in the analogue carboxamides.

A favorable change in the SAR was observed for the smaller compounds of this study. The most substantial change in activity was observed for compound **3**, which has a K_i of 789 nM against AmpC. Its exact carboxamide analogue **3c** is 23-fold less potent (18.5 μM). The high affinity of **3** corresponds

to a ligand efficiency of 0.91, placing it among the most efficient of enzyme inhibitors. Given the simplicity of this inhibitor, it seems clear that its improved affinity can be laid at the door of the advantages of the sulfonamide versus the carboxamide group in the AmpC site; this in turn may reflect the improved hydrogen bonds in this site owing to differences in polarity and geometry. This advantage was maintained during the SAR development among the smaller sulfonamide analogues, with potency improving 11-fold in compound **4** (K_i = 70 nM) and by another 3-fold in compound **9** (K_i = 25 nM). The X-ray complexes of these inhibitors underscore the favorable hydrogen bonds made between them and canonical recognition residues.

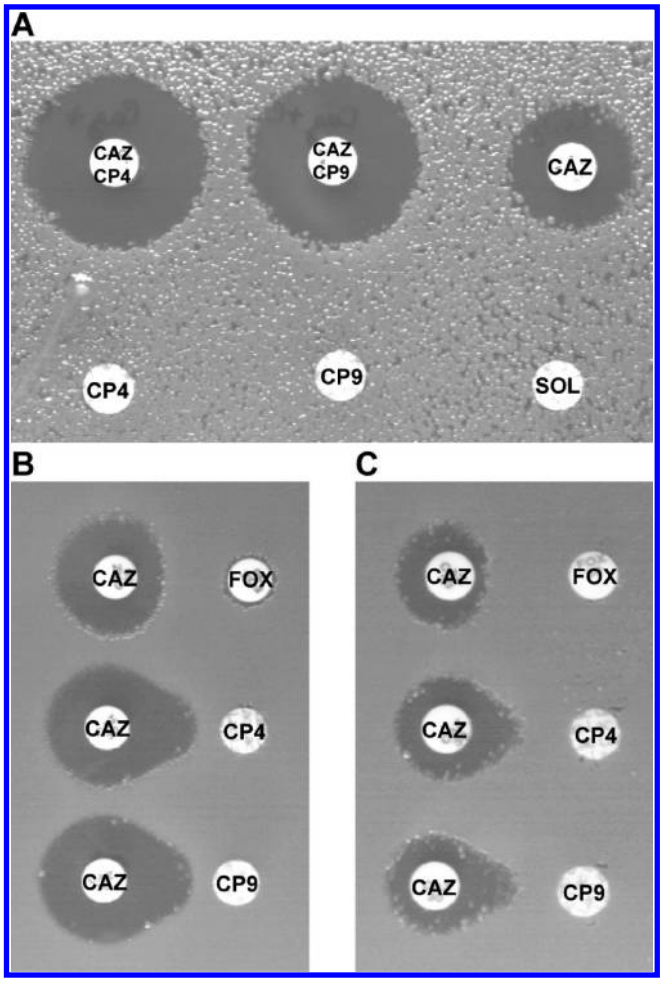

Figure 6. Inhibition of bacterial growth and potentiation effect. (A) Activity of compounds **4** (CP4) and **9** (CP9) in combination with ceftazidime (CAZ) and alone against a *Klebsiella pneumoniae* strain producing AmpC β-lactamase. Solvent (SOL) was DMSO/water 1:1. (B) Potentiation of β-lactamase inhibition in an *E. cloacae* strain in which *ampC* gene expression is inducible by β-lactam antibiotics, such as cefoxitin (FOX). (C) Potentiation of β-lactamase inhibition in a *Klebsiella pneumoniae* isolate producing the inducible class C enzyme DHA-1.

Conversely, in larger sulfonamides the SAR is inverted with affinities generally getting worse and relative to the carboxamides getting much worse. An example for the inversed SAR is the low affinity of the sulfonamide with the nafcillin side chain. Compound **11** is a 670 nM inhibitor compared to the carboxamide analogue **11c** with a K_i of 33 nM. This result suggests that adding a bulky side chain to the sulfonamide weakens, if not completely disrupts, the hydrogen bonds with residues Asn152 and Gln120 observed in the crystal structures of compounds **4** and **9**. Favorable stacking and van der Waals interaction of the elaborated aryl side chain may also be affected negatively.

We observed another change in the SAR when we tested compounds **16** and **17**, having a benzyl and *m*-carboxybenzyl as R_2 group, respectively. In the carboxamide boronic acids, adding a *m*-carboxybenzyl improved affinity 8-fold from compound **10c** to **17c**. In our sulfonamide series, the same modification (compound **4** to **17**) leads to a 6-fold drop in potency. In the structure of the AmpC/**17** complex, the sulfonamide hydrogen bonds have been completely disrupted and rearranged versus those made by **4** and **9** (Figure 5E). To understand the flip of the sulfonamide, we modeled compound **17** in the conformation observed for compound **4** (Figure 5F). The protein−inhibitor interactions in this model looked quite reasonable, but the ligand internal interactions were strained, with the aliphatic carbon in the *m*-carboxybenzyl group very close to one of the sulfonamide oxygens (3.0 Å). We reasoned that internal 1,5 repulsion between those two atoms could force the reorientation of the sulfonamide. We therefore calculated internal energies for both the model and the crystal structure of compound **17** using the semiempirical QM method AMSOL.[41] The internal energy of the ligand alone in the crystal structure conformation (−90.89 kcal/mol) was substantially lower than the internal energy of the modeled ligand (−55.08 kcal/mol), consistent with the internal strain hypothesis.

The unexpected SAR of these inhibitors suggests that we cannot simply adopt lessons learned from earlier series. Perhaps the most encouraging observation to emerge is that sulfonamide boronic acids with small R_1 side chains are very active against AmpC and can substantially reverse antibiotic resistance in bacterial cell culture. In addition, their activity against other β-lactamases classes, as shown here and by Tan et al.,[25] supports further studies on this new class of β-lactamase inhibitors.

Table 3. Minimum Inhibitory Concentrations of Third-Generation Cephalosporins Alone and in Association with Compound **4** or **9** (Ratio 1:1) for Clinical Bacteria Exhibiting a High Level of Resistance

	ceftazidime (μg/mL)	ceftazidime and **4** (μg/mL)	ceftazidime and **9** (μg/mL)	cefotaxime (μg/mL)	cefotaxime and **4** (μg/mL)	cefotaxime and **9** (μg/mL)
E. coli[a]	64	4	8	8	1	2
E. cloacae[a]	64	4	4	64	4	8
C. freundii[a]	64	4	4	16	2	4
P. aeruginosa[a]	32	4	8	>128	16	32
K. pneumoniae[b]	32	8	4	8	4	2
E. coli[c]	2	2	1	256	16	8

[a] Bacteria overproducing chromosomally mediated class C β-lactamase. [b] *K. pneumoniae* producing the plasmid-mediated class C β-lactamase DHA-1. [c] *E. coli* producing plasmid-mediated class A β-lactamase CTX-M-14.

Table 4. Selectivity of **4** and **9** for AmpC versus other Amide Hydrolases

enzyme	IC_{50} (μM) for **4**	IC_{50} (μM) for **9**
AmpC	0.38	0.13
CTX-M-9	6.87	1.50
α-chymotrypsin	>500[a]	>500[a]
cruzain	>500[a]	>500[a]

[a] No inhibition was observed at 100 μM. The IC_{50} values assume that inhibition was no greater than 20% at this concentration.

Methods

Synthesis and Analysis. All reactions were performed under argon using oven-dried glassware and dry solvents. Anhydrous tetrahydrofuran (THF) and diethyl ether were obtained by standard methods and freshly distilled under argon from sodium benzophenone ketyl prior to use. All reagents were purchased from Sigma-Aldrich and Fluka. The −100 °C bath was prepared by addition of liquid nitrogen to a precooled (−80 °C) mixture of ethanol/methanol (1:1). Reactions were monitored by TLC, which were visualized by UV fluorescence and by Hanessian's cerium molybdate stain. Chromatographic purification of the compounds was performed on silica gel (particle size 0.05−0.20 mm). Melting points were measured on a Büchi 510 apparatus. Optical rotations were recorded at +20 °C on a Perkin-Elmer 241 polarimeter and are expressed in 10^{-1} deg cm^2 g^{-1}. ^{1}H and ^{13}C NMR spectra were recorded on a Bruker DPX-200 or Avance-400 spectrometer. Chemical shifts (δ) are reported in ppm downfield from tetramethylsilane (TMS) as internal standard (s singlet, d doublet, t triplet, q quartet, m multiplet, br broad signal). Coupling constants (J) are given in Hz. Two-dimensional NMR techniques (COSY, HMBC, HSQC) were used to aid in the assignment of signals in ^{1}H and ^{13}C spectra. Mass spectra were determined on a gas chromatograph HP 5890 with mass spectrometer detector HP 5972 (EI, 70 eV) or on an Agilent Technologies LC−MS(n) ion trap 6310A. The purity of all tested compounds was above 95%, determined by elemental analysis performed on a Carlo Erba elemental analyzer 1110; results from elemental analyses for the compounds were within ±0.3% of the theoretical values. Data from MS fragmentation and elemental analyses of free boronic acids were not obtainable because of the formation of dehydration products. Nevertheless, these boronic acids could be converted into analytically pure pinacol/pinanediol esters by exposure to an equimolar amount of pinacol/pinanediol in anhydrous THF.

General Procedure for the Synthesis of Sulfonylaminomethaneboronates (3−6, 8, 11).[42] A solution of **2**[19] (1.00 mmol) in THF (3 mL) was added to a solution of anhydrous methanol in THF (2.5 M, 1.00 mmol) at −10 °C under argon flow. After being stirred for 10 min at −10 °C, the cooling bath was removed. The reaction mixture was stirred for 1 h at room temperature. Thereafter, the reaction mixture was cooled again to −10 °C and a solution of the selected sulfonyl chloride (1.10 mmol) in THF (2 mL) was slowly added. The resulting mixture was allowed to warm to room temperature overnight. The solvent was evaporated in vacuo and the residue purified by chromatography (dichloromethane/diethyl ether 8:2 to methanol), affording the expected sulfonamides.

Pinacol (Methanesulfonylamino)methaneboronate (3). According to the general procedure described before, the compound was recovered as a colorless oil (78% yield). ^{1}H NMR (200 MHz, $CDCl_3$): δ 1.26 (12H, s, pinacol protons), 2.79 (2H, d, J = 4.8, BCH_2), 2.91 (3H, s, CH_3S), 4.45 (1H, br, SO_2NH). ^{13}C NMR (100 MHz, $CDCl_3$): δ 24.8, 28.0 (*C*B), 38.6, 84.8. EI-MS, m/z: 220 (M^+ −15, 7%), 171 (29), 156 (24), 143 (21), 136 (39), 119 (14), 104 (100), 103 (44), 83 (37), 74 (6). Anal. Calcd for $C_8H_{18}BNO_4S$: C, 40.87; H, 7.72; N, 5.96; S, 13.64. Found: C, 41.02; H, 7.55; N, 5.77; S, 13.51.

Pinacol (Phenylmethanesulfonylamino)methaneboronate (4). White solid (84% yield). Mp 138−141 °C. ^{1}H NMR (200 MHz, $CDCl_3$): δ 1.27 (12H, s, pinacol protons), 2.71 (2H, s, BCH_2), 4.40 (1H, br, SO_2NH), 4.27 (2H, s, PhCH_2), 7.39 (5H, s, H_{Arom}). ^{13}C NMR (50 MHz, $CDCl_3$): δ 24.7, 29.6 (*C*B), 57.3, 84.7, 128.6, 128.7, 129.6, 130.6. EI-MS, m/z: 311 (M^+, 2%), 156 (18), 120 (5), 106 (8), 104 (17), 92 (9), 91 (100), 74 (17), 65 (11), 59 (16). Anal. Calcd for $C_{14}H_{22}BNO_4S$: C, 54.03; H, 7.13; N, 4.50; S, 10.30. Found: C, 54.32; H, 7.30; N, 4.29; S, 10.55.

Pinacol (4-Methylbenzenesulfonylamino)methaneboronate (5). White solid (84% yield). Mp 103−105 °C. ^{1}H NMR (200 MHz, DMSO): δ 1.17 (12H, s, pinacol protons), 2.25 (2H, d, J = 5.5, BCH_2), 2.38 (3H, s, CH_3Ph), 7.06 (1H, t, J = 5.5, SO_2NH), 7.38 (2H, d, J = 8.2, H_3, H_5), 7.65 (2H, d, J = 8.2, H_2, H_6). ^{13}C NMR (50 MHz, $CDCl_3$): δ 21.4, 24.7, 27.6 (*C*B), 84.6, 127.5, 129.6, 135.8, 143.2. EI-MS, m/z: 296 (M^+−15, 15%), 282 (55), 253 (31), 212 (19), 180 (78), 166 (26), 156 (100), 155 (39), 151 (46), 143 (20), 140 (30), 139 (89), 137 (23), 91 (80), 85 (19), 83 (25), 74 (98), 73 (30), 65 (31), 59 (20), 55 (23). Anal. Calcd for $C_{14}H_{22}BNO_4S$: C, 54.03; H, 7.13; N, 4.50; S, 10.30. Found: C, 54.26; H, 7.24; N, 4.22; S, 10.38.

Pinacol (3-Nitrophenylmethanesulfonylamino)methaneboronate (6). Yellowish viscous oil (84% yield). ^{1}H NMR (400 MHz, $CDCl_3$): δ 1.29 (12H, s, pinacol protons), 2.80 (2H, d, J = 4.4, BCH_2), 4.39 (2H, s, PhCH_2), 4.44 (1H, t, J = 4.4, SO_2NH), 7.59 (1H, t, J = 8.0, H_5), 7.80 (1H, d, J = 8.0, H_6), 8.23 (1H, d, J = 8.0, H_4), 8.29 (1H, s, H_2). ^{13}C NMR (100 MHz, $CDCl_3$): δ 24.8, 28.3 (*C*B), 56.6, 84.9, 123.5, 125.5, 129.8, 131.8, 136.9, 148.3. EI-MS, m/z: 341 (M^+ − 15, 2%), 327 (2), 240 (8), 165 (8), 156 (24), 137 (11), 136 (100), 129 (8), 104 (54), 103 (14), 90 (52), 89 (32), 83 (36), 74 (34), 59 (38), 43 (15), 41 (19). Anal. Calcd for $C_{14}H_{21}BN_2O_6S$: C, 47.21; H, 5.94; N, 7.86; S, 9.00. Found: C, 47.35; H, 6.05; N, 7.73; S, 8.74.

Pinacol (3-Aminophenylmethanesulfonylamino)methaneboronate Hydrochloride (7). Palladium 10 wt % on activated carbon (51 mg, 40% w/w) was added to a solution of **6** (128 mg, 0.36 mmol) in ethyl acetate (4 mL) and allowed to react under hydrogen atmosphere for 16 h. The catalyst was filtered off, and the solvent was evaporated in vacuo. The crude residue was dissolved in HCl (0.1 M solution in MeOH, 3.6 mL, 0.36 mmol). After 45 min the mixture was concentrated under reduced pressure and the residue repeatedly washed with diethyl ether, affording **7** as a yellowish solid (118 mg, 90% yield). Mp 193−196 °C. ^{1}H NMR (400 MHz, DMSO): δ 1.23 (12H, s, pinacol protons), 2.59 (2H, d, J = 3.82, BCH_2), 4.37 (2H, s, PhCH_2), 6.76 (1H, br, SO_2NH), 7.30−7.36 (3H, m, H_{Arom}), 7.46 (1H, t, J = 7.60, H_{Arom}), 9.60−10.60 (3H, br, NH_3^+). ^{13}C NMR (100 MHz, DMSO): δ 25.0, 27.5 (*C*B), 55.9, 84.2, 122.8, 125.3, 130.1, 130.5, 132.7, 133.0. EI-MS, m/z: 326 (M^+, 5%), 156 (8), 107 (64), 106 (100), 104 (15), 77 (11), 59 (11), 41 (8). Anal. Calcd for $C_{14}H_{24}BClN_2O_4S$: C, 46.36; H, 6.67; N, 7.72; S, 8.84. Found: C, 46.41; H, 6.50; N, 7.55; S, 8.68.

Pinacol [4-(Methoxycarbonyl)phenylmethanesufonylamino]methaneboronate (8). According to the general procedure described above, the compound was recovered as a white solid (84% yield). Mp 104−107 °C. ^{1}H NMR (400 MHz, $CDCl_3$): δ 1.27 (12H, s, pinacol protons), 2.73 (2H, d, J = 4.1, BCH_2), 3.93 (3H, s, COOCH_3), 4.33 (2H, s, PhCH_2), 4.37 (1H, br, SO_2NH), 7.49 (2H, d, J = 8.3, H_2, H_6), 8.04 (2H, d, J = 8.3, H_3, H_5). ^{13}C NMR (100 MHz, $CDCl_3$): δ 24.8, 28.4 (*C*B), 52.2, 57.2, 84.8, 129.9, 130.3, 130.7, 134.6, 166.6. EI-MS, m/z: 354 (M^+ − 15, < 2%), 338 (2), 311(2), 269 (3), 156 (25), 150 (24), 149 (100), 121 (24), 118 (13), 104 (19), 90 (19), 74 (26), 59 (13), 41 (9). Anal. Calcd for $C_{16}H_{24}BNO_6S$: C, 52.04; H, 6.55; N, 3.79; S, 8.68. Found: C, 51.88; H, 6.74; N, 3.56; S, 8.51.

[(4-Carboxyphenyl)methanesulfonylamino]methaneboronic Acid (9). A mixture of **8** (67 mg, 0.18 mmol) and HCl 3 N degassed (3 mL) was allowed to react at reflux for 1 h 30 min. After cooling, the reaction mixture was diluted with water (15 mL) and washed twice with diethyl ether (2 × 20 mL). The aqueous phase was concentrated in vacuo, affording **9** as a yellow solid (42 mg, 86% yield). Mp 118−122 °C (dec). ^{1}H NMR (400 MHz, DMSO): δ 2.5 (2H, d, J = 4.9, BCH_2), 4.42 (2H, s, PhCH_2), 6.22

(1H, t, J = 4.9, SO_2NH), 7.49 (2H, d, J = 8.6, H_2, H_6), 7.93 (2H, d, J = 8.6, H_3, H_5), 7.94 (1H, s, COO*H*). ^{13}C NMR (100 MHz, DMSO): δ 31.3 (*C*B), 55.7, 129.7, 130.7, 131.4, 136.0, 167.6. EI-MS and elemental analysis were not obtainable, but exposure of **9** to an equimolar amount of pinacol in anhydrous THF afforded the corresponding pinacol boronate in quantitative yield and satisfactory elemental analysis results. Anal. Calcd for $C_{15}H_{22}BNO_6S$: C, 50.72; H, 6.24; N, 3.94; S, 9.03. Found: C, 50.88; H, 6.41; N, 3.80; S, 8.77.

(2-Ethoxynaphthalene-1-sulfonylamino)methaneboronic Acid (11). According to the general procedure described above, reaction of **2** with 2-ethoxynaphthalene-1-sulfonyl chloride, obtained from 2-ethoxy-naphtalene,[43] afforded **11** as white solid free boronic acid (80% yield). ^{1}H NMR (200 MHz, MeOD): δ 1.46 (3H, t, J = 6.9, OCH_2CH_3), 1.94 (2H, s, BCH_2), 4.19 (2H, q, J = 6.9, OCH_2CH_3), 7.24 (1H, dd, J = 9.0, 2.0, H_{Arom}), 7.29 (1H, s, H_{Arom}), 7.70−7.91 (3H, m, H_{Arom}), 8.32 (1H, s, H_{Arom}). ^{13}C NMR (50 MHz, MeOD): δ 13.6, 20.7 (*C*B), 63.4, 106.2, 120.1, 123.2, 127.3, 127.4, 127.9, 130.1, 133.8, 136.4, 159.0. EI-MS and elemental analysis were not obtainable, but exposure of **11** to an equimolar amount of pinacol in anhydrous THF afforded the corresponding pinacol boronate in quantitative yield and satisfactory elemental analysis. Anal. Calcd for $C_{19}H_{26}BNO_5S$: C, 58.32; H, 6.70; N, 3.58; S, 8.19. Found: C, 58.19; H, 6.84; N, 3.40; S, 7.96.

(+)-Pinanediol 3-(*tert*-Butoxycarbonyl)benzeneboronate (12b). A solution of *tert*-butyl 3-bromobenzoate (1.70 g, 6.61 mmol), obtained from 3-bromobenzoic acid,[44] and freshly distilled triisopropyl borate (1.53 mL, 6.61 mmol) in THF (17 mL) was cooled to −100 °C under argon flow, and *n*-butyllithium (2.5 M solution in hexane, 2.91 mL, 7.27 mmol) was added dropwise over 15 min, during which the solution turned cherry red. After 1 h at −100 °C, trimethylsilyl chloride (0.84 mL, 6.61 mmol) was dropped into the reactor and the resulting colorless solution was allowed to warm to room temperature and stirred overnight. Finally, (+)-pinanediol (1.12 g, 6.61 mmol) was added and the solution stirred 1 h at room temperature. The mixture was partitioned between ethyl acetate (100 mL) and water (40 mL), and the aqueous phase was extracted with ethyl acetate (2 × 50 mL). The combined organic phases were washed with brine, dried over $MgSO_4$, filtered, and concentrated in vacuo. The crude residue was purified by column chromatography (light petroleum/ethyl ether 95:5), affording **12b** as a yellowish solid (2.10 g, 89% yield). Mp 70−71 °C. $[\alpha]_D$ +7.3 (*c* 1.1, $CHCl_3$). ^{1}H NMR (400 MHz, $CDCl_3$): δ 0.94 (3H, s, pinanyl CH_3), 1.24 (1H, d, J = 10.9, pinanyl H_{endo}), 1.36 (3H, s, pinanyl CH_3), 1.53 (3H, s, pinanyl CH_3), 1.64 (9H, s, *t*-Bu), 1.98−2.30 (5H, m, pinanyl protons), 4.51 (1H, dd, J = 8.5, 2.0, C*H*OB), 7.46 (1H, t, J = 7.6, H_5), 8.0 (1H, d, J = 7.6, H_4), 8.12 (1H, d, J = 7.6, H_6), 8.45 (1H, s, H_2). ^{13}C NMR (100 MHz, $CDCl_3$): δ 24.0, 26.5, 27.1, 28.2, 28.7, 35.5, 38.2, 39.5, 51.4, 78.4, 80.9, 86.5, 127.6, 131.5, 132.1, 135.7, 138.7, 169.5, *C*B not seen. EI-MS: m/z 356 (M^+, 10%), 300 (36), 283 (41), 231 (50), 204 (38), 83 (65), 67 (59), 57 (100). Anal. Calcd for $C_{21}H_{29}BO_4$: C, 70.80; H, 8.20. Found: C, 70.55; H, 8.22.

(+)-Pinanediol Phenylmethaneboronate (13a). *n*-Butyllithium (2.5 M solution in hexane, 4.66 mL, 11.64 mmol) was added dropwise to a stirred solution of (+)-pinanediol benzeneboronate **12a**[21] (2.48 g, 9.70 mmol) and bromochloromethane (0.95 mL, 14.55 mmol) in THF (25 mL) at −80 °C under argon atmosphere. The mixture was allowed to reach room temperature overnight. Then the solution was partitioned between light petroleum (80 mL) and water (25 mL), the organic phase was washed with saturated ammonium chloride (20 mL), and the combined aqueous phases were extracted with petroleum ether (2 × 40 mL). The organic phases were dried, filtered, and concentrated, and the crude residue was purified by gradient chromatography (light petroleum to light petroleum/ethyl ether 95:5), affording **13a** as a colorless oil (2.33 g, 89% yield). $[\alpha]_D$ +14.2 (*c* 2.0, $CHCl_3$). ^{1}H NMR (200 MHz, $CDCl_3$): δ 0.87 (3H, s, pinanyl CH_3), 1.10 (1H, d, J = 10.8, pinanyl H_{endo}), 1.30 (3H, s, pinanyl CH_3), 1.41 (3H, s, pinanyl CH_3), 1.62−2.39 (5H, m, pinanyl protons), 2.37 (2H, s, BCH_2), 4.30 (1H, dd, J = 8.8, 1.9, C*H*OB), 7.10−7.31 (5H, m, H_{Ar}). ^{13}C NMR (50 MHz, $CDCl_3$): δ 19.3 (*C*B), 24.0, 26.4, 27.1, 28.6, 35.5, 38.1, 39.5, 51.3, 78.0, 85.8, 124.8, 128.3, 128.9, 138.8. EI-MS: m/z 217 (M^+ + 1, 2%), 270 (M^+, 81%), 269 (M^+ − 1, 21%), 255 (32), 229 (24), 214 (32), 201 (88), 200 (33), 187 (30), 179 (28), 174 (100), 135 (58), 134 (38), 119 (32), 118 (26), 117 (28), 109 (24), 93 (44), 91 (74), 83 (75), 82 (32), 81 (34), 79 (24), 77 (26), 67 (66), 65 (27), 55 (47), 53 (29). Anal. Calcd for $C_{17}H_{23}BO_2$: C, 75.57; H, 8.58. Found: C, 75.39; H, 8.44.

(+)-Pinanediol [3-(*tert*-Butoxycarbonyl)phenyl]methaneboronate (13b). Following the procedure described for the synthesis of **13a**, compound **13b** was recovered from **12b** as a yellow oil (88% yield). $[\alpha]_D$ +8.7 (*c* 1.4, $CHCl_3$). ^{1}H NMR (400 MHz, $CDCl_3$): δ 0.87 (3H, s, pinanyl CH_3), 1.11 (1H, d, J = 11.0, pinanyl H_{endo}), 1.32 (3H, s, pinanyl CH_3), 1.43 (3H, s, pinanyl CH_3), 1.63 (9H, s, *t*-Bu), 1.84−2.39 (5H, m, pinanyl protons), 2.42 (2H, s, BCH_2), 4.32 (1H, dd, J = 8.8, 2.0, C*H*OB), 7.33 (1H, t, J = 7.7, H_5), 7.40 (1H, d, J = 7.7, H_6), 7.80 (1H, d, J = 7.7, H_4), 7.86 (1H, s, H_2). ^{13}C NMR (100 MHz, $CDCl_3$): δ 19.3 (*C*B), 24.0, 26.5, 27.1, 28.2, 28.6, 35.4, 38.2, 39.5, 51.3, 78.0, 80.7, 86.0, 126.2, 128.1, 129.9, 132.0, 133.2, 139.0, 166.0. EI-MS: m/z 370 (M^+, 18%), 314 (71), 297 (59), 135 (55), 57 (100). Anal. Calcd for $C_{22}H_{31}BO_4$: C, 71.36; H, 8.44. Found: C, 71.60; H, 8.27.

(+)-Pinanediol (1*R*)-1-(*N*-Bis(trimethylsilyl)amino)-2-phenylethaneboronate (14a). *n*-Butyllithium (2.5 M solution in hexane, 1.78 mL, 4.44 mmol) was added dropwise to a stirred solution of dichloromethane (0.36 mL, 5.55 mmol) in THF (8 mL) at −100 °C under argon atmosphere. At the end of the butyllithium addition, a white microcrystalline precipitate ($LiCHCl_2$) became evident. After 30 min, a solution of **13a** (1.00 g, 3.70 mmol) in THF (8 mL) was slowly added at the same temperature. The white precipitate disappeared, and the mixture was allowed to gradually reach room temperature overnight. The resulting solution was concentrated under reduced pressure. The crude was treated with petroleum ether (50 mL), and the resulting white inorganic precipitate was filtered off and washed with abundant petroleum ether. Solvent evaporation in vacuo afforded (+)-pinanediol (1*S*)-1-chloro-2-phenylethaneboronate, used as such for the subsequent reaction.

The above product was dissolved in THF (10 mL), and lithium bis(trimethylsilyl)amide (1.0 M solution in tetrahydrofuran, 3.70 mL, 3.70 mmol) was added dropwise at −100 °C under argon flow. The reaction mixture was allowed to reach room temperature overnight. The resulting solution was concentrated under reduced pressure, and the crude was treated with petroleum ether (50 mL). The white inorganic precipitate (LiCl) was filtered off and washed with abundant petroleum ether. The solvent was evaporated in vacuo to give a residue which was subjected to column chromatography (light petroleum/ethyl ether/triethylamine 98:2:5) recovering **14a** as a pale yellow oil (837 mg, 51% yield). $[\alpha]_D$ −14.8 (*c* 2.3, $CHCl_3$). ^{1}H NMR (400 MHz, $CDCl_3$): δ 0.12 (18H, s, $2Si(CH_3)_3$), 0.87 (3H, s, pinanyl CH_3), 0.99 (1H, d, J = 10.8, pinanyl H_{endo}), 1.31 (3H, s, pinanyl CH_3), 1.41 (3H, s, pinanyl CH_3), 1.78−2.36 (5H, m, pinanyl protons), 2.71 (1H, dd, J = 13.1, 7.6, $CHCH_2$), 2.87 (1H, t, J = 7.4, BCH), 3.08 (1H, dd, J = 13.1, 7.3, $CHCH_2$), 4.31 (1H, dd, J = 8.7, 2.0, C*H*OB), 7.17−7.31 (5H, m, H_{Arom}). ^{13}C NMR (100 MHz, $CDCl_3$): δ 3.0, 24.0, 26.0, 27.1, 28.4, 35.2, 38.1, 39.5, 42.0, 45.0 (*C*B), 51.4, 78.2, 85.6, 125.7, 127.8, 129.7, 141.7. Anal. Calcd for $C_{24}H_{42}BNO_2Si_2$: C, 64.98; H, 9.54; N, 3.16. Found: C, 65.19; H, 9.46; N, 2.95.

(+)-Pinanediol (1*R*)-2-(3(*tert*-Butoxycarbonyl)phenyl)-1-(*N*-bis(trimethylsilyl)amino)ethaneboronate (14b). Following the procedure described for the synthesis of **14a**, compound **14b** was recovered as a colorless oil (28% yield). $[\alpha]_D$ −12.6 (*c* 3.9, $CHCl_3$). ^{1}H NMR (200 MHz, $CDCl_3$): δ 0.10 (18H, s, $2Si(CH_3)_3$), 0.83 (3H, s, pinanyl CH_3), 0.94 (1H, d, J = 11.1,

pinanyl H_{endo}), 1.28 (3H, s, pinanyl CH_3), 1.38 (3H, s, pinanyl CH_3), 1.61 (9H, s, *t*-Bu), 1.78−2.35 (5H, m, pinanyl protons), 2.66−2.87 (2H, m, BC*H*, CHCH_2), 3.06−3.15 (1H, m, CHCH_2), 4.29 (1H, d, J = 8.7, C*H*OB), 7.29−7.43 (2H, m, H_5, H_6), 7.82−7.91 (2H, m, H_2, H_4). ^{13}C NMR (50 MHz, $CDCl_3$): δ 3.0, 23.9, 26.2, 27.0, 28.2, 28.4, 35.1, 38.1, 39.5, 41.8, 44.8 (*C*B), 51.4, 78.3, 80.5, 85.6, 126.9, 127.7, 130.8, 131.5, 133.8, 141.7, 166.0. Anal. Calcd for $C_{29}H_{50}BNO_4Si_2$: C, 64.06; H, 9.27; N, 2.58. Found: C, 63.84; H, 9.06; N, 2.77.

(+)-Pinanediol (1*R*)-1-(Phenylmethanesulfonylamino)-2-phenylethaneboronate (15a). A solution of **14a** (840 mg, 1.89 mmol) in THF (2 mL) was added to a THF solution of anhydrous methanol (2.5 M, 0.76 mL, 1.89 mmol) at −10 °C under nitrogen and magnetically stirred for 10 min at −10 °C. The cooling bath was removed, and the solution was stirred at room temperature for an additional hour. Thereafter, the temperature was lowered to −40 °C and phenylmethanesulfonyl chloride (469 mg, 2.46 mmol) in THF (2 mL) was slowly dropped in. The resulting colorless solution was allowed to gradually reach room temperature and stirred overnight. The solution was partitioned between diethyl ether (30 mL) and water (10 mL). The aqueous phase was extracted with diethyl ether (2 × 20 mL), and the combined organic phases were dried (Na_2SO_4), filtered, and concentrated. The crude residue was purified by column chromatography (dichloromethane/diethyl ether 6:4), affording **15a** as a thick yellowish oil (343 mg, 40% yield). $[\alpha]_D$ +9.7 (*c* 1.6, $CHCl_3$). ^{1}H NMR (400 MHz, $CDCl_3$): δ 0.85 (3H, s, pinanyl CH_3), 1.10 (1H, d, J = 10.8, pinanyl H_{endo}), 1.31 (3H, s, pinanyl CH_3), 1.32 (3H, s, pinanyl CH_3), 1.82−2.42 (5H, m, pinanyl protons), 2.90 (1H, dd, J = 13.7, 7.1, CHCH_2), 3.08 (1H, dd, J = 13.7, 5.5, CHCH_2), 3.27−3.39 (1H, m, BC*H*), 4.18 (1H, br, SO_2N*H*), 4.21 (2H, s, CH_2SO_2), 4.35 (1H, dd, J = 8.8, 2.0, C*H*OB), 7.20−7.34 (10H, m, H_{Arom}). ^{13}C NMR (100 MHz, $CDCl_3$): δ 23.9, 26.3, 27.0, 28.3, 35.1, 38.1, 38.8, 39.4, 42.5 (*C*B), 51.2, 59.1, 78.6, 86.9, 126.6, 128.4, 128.5, 128.6, 129.6, 129.7, 130.7, 138.4. Anal. Calcd for $C_{25}H_{32}BNO_4S$: C, 66.23; H, 7.11; N, 3.09; S 7.07. Found: C, 66.04; H, 6.97; N, 2.88; S, 6.91.

Pinanediol (1*R*)-2-(3(*tert*-Butoxycarbonyl)phenyl)-1-(phenylmethanesulfonylamino)ethaneboronate (15b). Following the procedure described for **15a**, compound **15b** was recovered as a yellowish oil (35% yield). $[\alpha]_D$ +18.7 (*c* 0.7, $CHCl_3$). ^{1}H NMR (400 MHz, $CDCl_3$): δ 0.82 (3H, s, pinanyl CH_3), 1.00 (1H, d, J = 10.9, pinanyl H_{endo}), 1.26 (3H, s, pinanyl CH_3), 1.28 (3H, s, pinanyl CH_3), 1.59 (9H, s, *t*-Bu), 1.83−2.36 (5H, m, pinanyl protons), 2.95 (1H, dd, J = 13.3, 6.4, CHCH_2), 3.10 (1H, dd, J = 13.3, 5.6, CHCH_2), 3.31 (1H, q, J = 5.9, BC*H*), 4.17 (1H, d, J = 5.9, SO_2N*H*), 4.23 (2H, s, CH_2SO_2), 4.37 (1H, d, J = 8.7, 2.0, C*H*OB), 7.32−7.44 (7H, m, H_{Arom}), 7.83−7.85 (2H, m, H_{Arom}). ^{13}C NMR (100 MHz, $CDCl_3$): δ 24.0, 26.3, 27.0, 28.2, 29.7, 35.0, 38.2, 38.7, 39.4, 42.5 (*C*B), 51.1, 59.1, 78.7, 81.0, 87.1, 127.8, 128.5, 129.0, 129.1, 129.6, 130.4, 130.8, 132.1, 134.1, 138.5, 165.7. Anal. Calcd for $C_{30}H_{40}BNO_6S$: C, 65.10; H, 7.28; N, 2.53; S 5.79. Found: C, 64.88; H, 7.02; N, 2.29; S, 5.47.

(1*R*)-1-(Phenylmethanesulfonylamino)-2-phenylethaneboronic Acid (16). To a solution of **15a** (245 mg, 0.54 mmol) in CH_3CN (3 mL) were sequentially added HCl (1 M aqueous solution, 350 μL, 0.35 mmol), phenylboronic acid (62 mg, 0.51 mmol), and *n*-hexane (3 mL). The resulting biphasic solution was vigorously stirred. After 30 min the *n*-hexane layer, containing the pinanediol phenylboronate, was removed and fresh *n*-hexane (3 mL) was added. This last procedure was repeated several times until a TLC analysis revealed no remaining pinanediol boronate. The acetonitrile phase was then concentrated affording **16** as a yellowish solid (159 mg, 92% yield). Mp 107 °C (dec). $[\alpha]_D$ +78.0 (*c* 1.0, MeOH). ^{1}H NMR (400 MHz, MeOD): δ 2.83 (2H, d, J = 7.1, CHCH_2), 3.05 (1H, t, J = 7.1, BC*H*), 4.20 (2H, s, CH_2SO_2), 7.16−7.44 (10H, m, H_{Arom}). ^{13}C NMR (100 MHz, MeOD): δ 38.8, 39.3 (*C*B), 58.6, 126.1, 127.2, 128.0, 128.2, 129.0, 130.1, 130.6, 133.3. EI-MS and elemental analysis results were not obtainable, but exposure of **16** to an equimolar amount of (+)-pinanediol in anhydrous THF afforded compound **15a** in quantitative yield and satisfactory elemental analysis results. Anal. Calcd for $C_{25}H_{32}BNO_4S$: C, 66.23; H, 7.11; N, 3.09; S 7.07. Found: C, 66.14; H, 6.91; N, 3.32; S, 6.89.

(1*R*)-2-(3-Carboxyphenyl)-1-(phenylmethanesulfonylamino)-ethaneboronic Acid (17). A solution of **15b** (90 mg, 0.16 mmol) in dichloromethane (2 mL) was cooled to −10 °C and treated with an excess of trifluoroacetic acid (10% v/v solution in dichloromethane, 2 mL). After 10 min at −10 °C, the mixture was allowed to react at room temperature for 5 h. The solution was concentrated in vacuo and the residue crystallized from diethyl ether, affording (+)-pinanediol (1*R*)-2-[3-carboxyphenyl]-1-(phenylmethanesulfonylamino)ethaneboronate (79 mg, 100% yield) as a cream colored solid. Mp 155−158 °C. $[\alpha]_D$ +25.9 (*c* 0.6, $CHCl_3$). ^{1}H NMR (400 MHz, $CDCl_3$): δ 0.87 (3H, s, pinanyl CH_3), 1.06 (1H, d, J= 10.8, pinanyl H_{endo}), 1.31 (3H, s, pinanyl CH_3), 1.33 (3H, s, pinanyl CH_3), 1.88−2.38 (5H, m, pinanyl protons), 2.99 (1H, dd, J = 13.7, 6.0, CHCH_2), 3.15 (1H, dd, J = 13.7, 5.6, CHCH_2), 3.37 (1H, br, BC*H*), 4.31 (2H, s, CH_2SO_2), 4.40 (1H, d, J= 7.7, C*H*OB), 4.51 (1H, br, SO_2N*H*), 7.30−7.58 (7H, m, H_{Arom}), 7.97−8.01 (2H, m, H_{Arom}), 10.2 (1H, br, COO*H*). ^{13}C NMR (100 MHz, $CDCl_3$): δ 24.0, 26.3, 27.0, 28.3, 35.0, 38.2, 38.5, 39.4, 42.4 (*C*B), 51.1, 59.2, 78.8, 87.3, 128.5, 128.6, 128.7, 127.2, 129.3, 129.4, 130.8, 131.2, 135.6, 139.0, 171.8. Anal. Calcd for $C_{26}H_{32}BNO_6S$: C, 62.78; H, 6.48; N, 2.82; S 6.45. Found: C, 62.61; H, 6.72; N, 2.64; S, 6.21.

This compound was then treated according to the procedure described for **16** to recover **17** as a yellowish solid (54 mg, 92% yield). Mp 118−122 °C (dec). $[\alpha]_D$ +136.0 (*c* 0.5, MeOH). ^{1}H NMR (400 MHz, MeOD): δ 2.87 (2H, d, J = 7.0, CHCH_2), 3.05 (1H, t, J = 7.0, BC*H*), 4.24 (2H, s, CH_2SO_2), 7.31−7.88 (9H, m, H_{Arom}). ^{13}C NMR (100 MHz, MeOD): δ 38.4, 42.9 (*C*B), 58.8, 127.5, 128.0, 128.1, 128.2, 129.6, 130.1, 130.2, 130.6, 133.8, 139.1, 168.4. EI-MS and elemental analysis were not obtainable, but exposure of **11** to an equimolar amount of (+)-pinanediol in anhydrous THF afforded the corresponding pinanediol boronate in quantitative yield and satisfactory elemental analysis. Anal. Calcd for $C_{26}H_{32}BNO_6S$: C, 62.78; H, 6.48; N, 2.82; S 6.45. Found: C, 62.56; H, 6.71; N, 2.59; S, 6.28.

Enzymology. Sulfonamidomethaneboronic acids were dissolved in 100% DMSO at 100 mM. More diluted stocks were prepared as necessary. AmpC activity was determined by monitoring the change of absorbance at 405 nm due to hydrolyzed substrate CENTA (K_m = 15 μM) by an HP5453 UV−vis spectrophotometer. The enzyme was expressed and purified as described,[45] and CENTA was purchased from Tydock Pharma.

Kinetic measurements were run at room temperature in 50 mM sodium cacodylate, pH 6.5, in the presence of 0.01% Triton-X to prevent nonspecific inhibition via compound aggregation.[46,47] These conditions also ensure the hydrolysis of pinacol esters to free boronic acids.[48] Reactions were performed in 1 mL cuvettes with 60 μM CENTA and initiated by adding 1.2 nM enzyme. No incubation effect was detected for any compound, consistent with earlier studies.[18] The first 180 s of each reaction was used to measure initial rates. IC_{50} values were obtained by fitting binding data to a sigmoidal dose−response equation using GraphPad Prism (GraphPad software, Inc.). K_i values were determined by the use of the Cheng−Prusoff equation.[49]

The selectivity of compounds **4** and **9** was tested by determining their activity against CTX-M-9 β-lactamase, α-chymotrypsin (bovine pancreatic), and cruzain. α-Chymotrypsin and all necessary assay components were purchased from Sigma-Aldrich. Recombinant cruzain was provided by Dr. Rafaela Ferreira and CTX-M-9 by Dr. Yu Chen.

CTX-M-9 activity was measured under the same conditions as with AmpC, with 60 μM CENTA (K_m = 35 μM) as substrate. Reactions were initiated by the addition of 0.3 nM enzyme and monitored at 405 nm.

α-Chymotrypsin assays were performed in 50 mM Tris buffer, pH 7.5, with 0.01% Triton-X. Inhibitor and 0.001 mg/mL enzyme were incubated at their final concentration for 10 min before the reaction was initiated by the addition of 200 μM *N*-succinyl-Ala-Ala-Pro-Phe *p*-nitroanilide and monitored at 410 nm.

Cruzain assays were performed in 100 mM sodium acetate, pH 5.5, with 0.01% Triton-X and 5 mM dithiothreitol. Cruzain activity was measured in a 96-well format fluorimetric assay, monitoring the cleavage of the substrate Z-Phe-Arg-aminomethylcoumarin (Z-FR-AMC), in a SpectraMax M5 Molecular Devices spectrofluorimeter. Inhibitor and 0.4 nM enzyme were incubated at their final concentration for 10 min before the reactions were initiated by the addition of 2.5 μM Z-FR-AMC (K_m = 2 μM) and monitored for 5 min, determining activity based on initial rates.

Modeling. Compound **17** was modeled in complex with AmpC by superposing **17** on the crystal structure of compound **4** in chain A. To remove clashes of the additional *m*-carboxybenzyl group with the protein, we minimized **17** in the AmpC active site by an all-atom energy minimization using PLOP.[50] The oxygen atom of Ser64 was allowed to move while the rest of the enzyme was kept rigid during the minimization. This resulted in a model with the phenylmethanesulfonamide conformation resembling the conformation observed for compounds **4** and **9**, in which the sulfonamide oxygen atoms pointed in the direction of the *m*-carboxybenzyl group.

Crystal Growth and Structure Determination. Cocrystals of AmpC in complex with compound **4**, **9**, and **17** were grown by vapor diffusion in hanging drop vapor diffusion experiments equilibrated over 1.7 M potassium phosphate buffer (pH 8.7−8.9) using microseeding technique. The initial concentration of the protein was 3.9 mg/mL. The concentrations of the compounds were 625 μM, and the DMSO concentration was 1.25%. Crystals appeared 4−7 days after equilibration at 20 °C. Before data collection, crystals were immersed in a cryoprotectant solution of 25% sucrose, 1.7 M potassium phosphate, pH 8.7, for about 30 s and were flash-cooled in liquid nitrogen.

Diffraction data were measured at beamline 8.3.1 of the Advance Light Source (ALS, Lawrence Berkeley Lab, CA). Reflections were indexed, integrated, and scaled using the XDS package.[51] The space group was *C*2 with two molecules in the asymmetric unit. The initial phasing model was an apo AmpC model (PDB entry 1KE4), with water molecules and ions removed. The model was positioned initially by rigid body refinement and further refined with L-BFGS minimization, simulated annealing, individual *B*-factor refinement, and water picking using PHENIX.[52] Coot was used for model building, and the PRODRG server was used to generate ligand restraints.[53,54] Ligand restraints were modified manually because the PRODRG server does not support boron atoms.

Microbiology. Susceptibility testing was performed and interpreted following the guidelines of CLSI.[40] The compounds were dissolved in 50% DMSO, and dilutions were performed using Muller−Hinton medium. An adequate final concentration was obtained to determine the minimum inhibitory concentrations (MICs). The concentration of DMSO was maintained below 5%. The inhibitors were tested for synergy with the third-generation β-lactams ceftazidime and cefotaxime against several clinical bacteria. The ratio of β-lactams to inhibitors was 1:1. Each value reported reflects the average of three independent experiments. The bacteria exhibited a high level of resistance to β-lactams because of the expression of class C or class A β-lactamases. One *Escherichia coli* strain showed an AmpC-overproduced phenotype, and the second one produced the plasmid-mediated class A β-lactamase CTX-M-14. *Citrobacter freundii*, *Enterobacter cloacae*, and *Pseudomas aeruginosa* strains showed AmpC-derepressed phenotype. *Klebsiella pneumoniae* isolate produced the inducible plasmid-metiated class C enzyme DHA-1.

For disk diffusion plate assays, bacterial strains were diluted in sterile water to a turbidity equivalent to 0.5 McFarland turbidity standards. After a subsequent 10-fold dilution, the bacterial suspensions were inoculated on Mueller−Hinton agar. The plates were dried for 10 min before applying the disks containing cefotaxime or ceftazidime antibiotics (30 μg) or the inhibitor (30 μg) or both. After overnight incubation at 37 °C, the zones of bacterial-growth inhibition were measured.

For the β-lactamase induction experiments, plates of Mueller−Hinton agar were inoculated with two clinical strains (*E. cloacae* and *K. pneumoniae*) in which production of AmpC-type enzyme is inducible by β-lactam antibiotics. Inhibitors were added to blank disks, and the final content of inhibitor per disk was 64 μg of compounds and 32 μg cefoxitin. Disks of ceftazidime contained 30 μg of antibiotic.

Acknowledgment. This work was supported by NIH Grant GM63815 (B.K.S. and F.P.), SNF Fellowship PBZHP3-123277 (O.E.), and Fondazione Cassa di Risparmio di Modena (F.P., C.R., and E.C.). We thank Drs. Magdalena Korczynska and Kristin Ziebart for reading this manuscript, Dr. Claudia Ori for analytical support, and the Centro Interdipartimentale Grandi Strumenti of Modena for NMR and MS spectra.

References

(1) Livermore, D. M. beta-Lactamases—the threat renews. *Curr. Protein Pept. Sci.* **2009**, *10*, 397–400.
(2) Fisher, J. F.; Meroueh, S. O.; Mobashery, S. Bacterial resistance to beta-lactam antibiotics: compelling opportunism, compelling opportunity. *Chem. Rev.* **2005**, *105*, 395–424.
(3) Paterson, D. L.; Bonomo, R. A. Extended-spectrum beta-lactamases: a clinical update. *Clin. Microbiol. Rev.* **2005**, *18*, 657–686.
(4) Wilke, M. S.; Lovering, A. L.; Strynadka, N. C. Beta-lactam antibiotic resistance: a current structural perspective. *Curr. Opin. Microbiol.* **2005**, *8*, 525–533.
(5) Lode, H. M. Rational antibiotic therapy and the position of ampicillin/sulbactam. *Int. J. Antimicrob. Agents* **2008**, *32*, 10–28.
(6) Drawz, S. M.; Bonomo, R. A. Three decades of beta-lactamase inhibitors. *Clin. Microbiol. Rev.* **2010**, *23*, 160–201.
(7) Bebrone, C.; Lassaux, P.; Vercheval, L.; Sohier, J. S.; Jehaes, A.; Sauvage, E.; Galleni, M. Current challenges in antimicrobial chemotherapy: focus on beta-lactamase inhibition. *Drugs* **2010**, *70*, 651–679.
(8) Bush, K. beta-Lactamases of increasing clinical importance. *Curr. Pharm. Des.* **1999**, *5*, 839–845.
(9) Jacoby, G. A. AmpC beta-lactamases. *Clin. Microbiol. Rev.* **2009**, *22*, 161–182.
(10) Vilar, M.; Galleni, M.; Solmajer, T.; Turk, B.; Frere, J. M.; Matagne, A. Kinetic study of two novel enantiomeric tricyclic beta-lactams which efficiently inactivate class C beta-lactamases. *Antimicrob. Agents Chemother.* **2001**, *45*, 2215–2223.
(11) Buynak, J. D. The discovery and development of modified penicillin- and cephalosporin-derived beta-lactamase inhibitors. *Curr. Med. Chem.* **2004**, *11*, 1951–1964.
(12) Buynak, J. D.; Chen, H.; Vogeti, L.; Gadhachanda, V. R.; Buchanan, C. A.; Palzkill, T.; Shaw, R. W.; Spencer, J.; Walsh, T. R. Penicillin-derived inhibitors that simultaneously target both metallo- and serine-beta-lactamases. *Bioorg. Med. Chem. Lett.* **2004**, *14*, 1299–1304.
(13) Plantan, I.; Selic, L.; Mesar, T.; Anderluh, P. S.; Oblak, M.; Prezelj, A.; Hesse, L.; Andrejasic, M.; Vilar, M.; Turk, D.; Kocijan, A.; Prevec, T.; Vilfan, G.; Kocjan, D.; Copar, A.; Urleb, U.; Solmajer, T. 4-Substituted trinems as broad spectrum beta-lactamase inhibitors: structure-based design, synthesis, and biological activity. *J. Med. Chem.* **2007**, *50*, 4113–4121.
(14) Strynadka, N. C.; Martin, R.; Jensen, S. E.; Gold, M.; Jones, J. B. Structure-based design of a potent transition state analogue for TEM-1 beta-lactamase. *Nat. Struct. Biol.* **1996**, *3*, 688–695.
(15) Lobkovsky, E.; Billings, E. M.; Moews, P. C.; Rahil, J.; Pratt, R. F.; Knox, J. R. Crystallographic structure of a phosphonate derivative of the *Enterobacter cloacae* P99 cephalosporinase: mechanistic interpretation of a beta-lactamase transition-state analog. *Biochemistry* **1994**, *33*, 6762–6772.
(16) Maveyraud, L.; Pratt, R. F.; Samama, J. P. Crystal structure of an acylation transition-state analog of the TEM-1 beta-lactamase.

Mechanistic implications for class A beta-lactamases. *Biochemistry* **1998**, *37*, 2622–2628.
(17) Powers, R. A.; Blazquez, J.; Weston, G. S.; Morosini, M. I.; Baquero, F.; Shoichet, B. K. The complexed structure and antimicrobial activity of a non-beta-lactam inhibitor of AmpC beta-lactamase. *Protein Sci.* **1999**, *8*, 2330–2337.
(18) Weston, G. S.; Blazquez, J.; Baquero, F.; Shoichet, B. K. Structure-based enhancement of boronic acid-based inhibitors of AmpC beta-lactamase. *J. Med. Chem.* **1998**, *41*, 4577–4586.
(19) Caselli, E.; Powers, R. A.; Blasczcak, L. C.; Wu, C. Y.; Prati, F.; Shoichet, B. K. Energetic, structural, and antimicrobial analyses of beta-lactam side chain recognition by beta-lactamases. *Chem. Biol.* **2001**, *8*, 17–31.
(20) Beadle, B. M.; Trehan, I.; Focia, P. J.; Shoichet, B. K. Structural milestones in the reaction pathway of an amide hydrolase: substrate, acyl, and product complexes of cephalothin with AmpC beta-lactamase. *Structure* **2002**, *10*, 413–424.
(21) Morandi, F.; Caselli, E.; Morandi, S.; Focia, P. J.; Blazquez, J.; Shoichet, B. K.; Prati, F. Nanomolar inhibitors of AmpC beta-lactamase. *J. Am. Chem. Soc.* **2003**, *125*, 685–695.
(22) Morandi, S.; Morandi, F.; Caselli, E.; Shoichet, B. K.; Prati, F. Structure-based optimization of cephalothin-analogue boronic acids as beta-lactamase inhibitors. *Bioorg. Med. Chem.* **2008**, *16*, 1195–1205.
(23) Powers, R. A.; Morandi, F.; Shoichet, B. K. Structure-based discovery of a novel, noncovalent inhibitor of AmpC beta-lactamase. *Structure* **2002**, *10*, 1013–1023.
(24) Sheehan, J. C.; Hoff, D. R. The synthesis of substituted penicillins and simpler structural analogs. XII. 6-benzylsulfonamidopenicillanic acid. *J. Am. Chem. Soc.* **1957**, *79*, 237–240.
(25) Tan, Q.; Ogawa, A. M.; Painter, R. E.; Park, Y. W.; Young, K.; DiNinno, F. P. 4,7-Dichloro benzothien-2-yl sulfonylaminomethyl boronic acid: first boronic acid-derived beta-lactamase inhibitor with class A, C, and D activity. *Bioorg. Med. Chem. Lett.* **2010**, *20*, 2622–2624.
(26) Walker, G.; Rana, K. K. A novel preparation of 2-naphthyl and 5-benzo[*b*]thienyl methanesulfonyl chlorides. *Synth. Commun.* **2003**, *33*, 627–632.
(27) Schlapbach, A.; Hoffmann, R. W. (*E*)-Alpha-sulfonamidocrotylboronates as reagents for the stereoselective homoaldol synthesis. *Eur. J. Org. Chem.* **2001**, 323–328.
(28) Hercouet, A.; Baudet, C.; Carboni, B. Synthesis of new boron analogues of cyclic carboxylic alpha-amino acids using ring-closing metathesis reactions. *Tetrahedron Lett.* **2004**, *45*, 8749–8751.
(29) Matteson, D. S. Functional group compatibilities in boronic ester chemistry. *J. Organomet. Chem.* **1999**, *581*, 51–65.
(30) Sadhu, K. M.; Matteson, D. S. (Chloromethyl)lithium: efficient generation and capture by boronic esters and a simple preparation of diisopropyl (chloromethyl)boronate. *Organometallics* **1985**, *4*, 1687–1689.
(31) Matteson, D. S.; Ray, R.; Rocks, R. R.; Tsai, D. J. S. Directed chiral synthesis by way of alpha-chloro boronic esters. *Organometallics* **1983**, *2*, 1536–1543.
(32) Matteson, D. S. Asymmetric synthesis with boronic esters. *Acc. Chem. Res.* **1988**, *21*, 294–300.
(33) Matteson, D. S. alpha-Halo boronic esters: intermediates for stereodirected synthesis. *Chem. Rev.* **1989**, *89*, 1535–1551.
(34) Wityak, J.; Earl, R. A.; Abelman, M. M.; Bethel, Y. B.; Fisher, B. N.; Kauffman, G. S.; Kettner, C. A.; Ma, P.; McMillan, J. L.; Mersinger, L. J.; Pesti, J.; Pierce, M. E.; Rankin, W. F.; Chorvat, R. J.; Confalone, P. N. Synthesis of thrombin inhibitor DuP 714. *J. Org. Chem.* **1995**, *60*, 3717–3722.
(35) Chen, Y.; McReynolds, A.; Shoichet, B. K. Re-examining the role of Lys67 in class C beta-lactamase catalysis. *Protein Sci.* **2009**, *18*, 662–669.
(36) Bulychev, A.; Mobashery, S. Class C beta-lactamases operate at the diffusion limit for turnover of their preferred cephalosporin substrates. *Antimicrob. Agents Chemother.* **1999**, *43*, 1743–1746.
(37) Patera, A.; Blaszczak, L. C.; Shoichet, B. K. Crystal structures of substrate and inhibitor complexes with AmpC beta-lactamase: possible implications for substrate-assisted catalysis. *J. Am. Chem. Soc.* **2000**, *122*, 10504–10512.
(38) Galleni, M.; Lamotte-Brasseur, J.; Raquet, X.; Dubus, A.; Monnaie, D.; Knox, J. R.; Frere, J. M. The enigmatic catalytic mechanism of active-site serine beta-lactamases. *Biochem. Pharmacol.* **1995**, *49*, 1171–1178.
(39) Rahil, J.; Pratt, R. F. Characterization of covalently bound enzyme inhibitors as transition-state analogs by protein stability measurements: phosphonate monoester inhibitors of a beta-lactamase. *Biochemistry* **1994**, *33*, 116–125.
(40) *Performance Standards for Antimicrobial Susceptibility Testing*; 20th Informational Supplement, M100-S20; Clinical and Laboratory Standards Institute: Wayne, PA, 2010.
(41) Cramer, C. J.; Truhlar, D. G. AM1-SM2 and PM3-SM3 parameterized SCF solvation models for free energies in aqueous solution. *J. Comput.-Aided Mol. Des.* **1992**, *6*, 629–666.
(42) Matteson, D. S.; Jesthi, P. K.; Sadhu, K. M. Synthesis and properties of pinanediol alpha-amido boronic esters. *Organometallics* **1984**, *3*, 1284–1288.
(43) Yekta, S.; Krasnova, L. B.; Mariampillai, B.; Picard, C. J.; Chen, G.; Pandiaraju, S.; Yudin, A. K. Preparation and catalytic applications of partially fluorinated binaphthol ligands. *J. Fluorine Chem.* **2004**, *125*, 517–525.
(44) Wright, S. W.; Hageman, D. L.; Wright, A. S.; McClure, L. D. Convenient preparations of *t*-butyl esters and ethers from t-butanol. *Tetrahedron Lett.* **1997**, *38*, 7345–7348.
(45) Usher, K. C.; Blaszczak, L. C.; Weston, G. S.; Shoichet, B. K.; Remington, S. J. Three-dimensional structure of AmpC beta-lactamase from *Escherichia coli* bound to a transition-state analogue: possible implications for the oxyanion hypothesis and for inhibitor design. *Biochemistry* **1998**, *37*, 16082–16092.
(46) Feng, B. Y.; Shelat, A.; Doman, T. N.; Guy, R. K.; Shoichet, B. K. High-throughput assays for promiscuous inhibitors. *Nat. Chem. Biol.* **2005**, *1*, 146–148.
(47) Feng, B. Y.; Simeonov, A.; Jadhav, A.; Babaoglu, K.; Inglese, J.; Shoichet, B. K.; Austin, C. P. A high-throughput screen for aggregation-based inhibition in a large compound library. *J. Med. Chem.* **2007**, *50*, 2385–2390.
(48) Kettner, C. A.; Shenvi, A. B. Inhibition of the serine proteases leukocyte elastase, pancreatic elastase, cathepsin G, and chymotrypsin by peptide boronic acids. *J. Biol. Chem.* **1984**, *259*, 15106–15114.
(49) Cheng, Y.; Prusoff, W. H. Relationship between the inhibition constant (K1) and the concentration of inhibitor which causes 50 per cent inhibition (I50) of an enzymatic reaction. *Biochem. Pharmacol.* **1973**, *22*, 3099–3108.
(50) Kalyanaraman, C.; Bernacki, K.; Jacobson, M. P. Virtual screening against highly charged active sites: identifying substrates of alpha-beta barrel enzymes. *Biochemistry* **2005**, *44*, 2059–2071.
(51) Kabsch, W. Automatic processing of rotation diffraction data from crystals of initially unknown symmetry and cell constants. *J. Appl. Crystallogr.* **1993**, *26*, 795–800.
(52) Adams, P. D.; Afonine, P. V.; Bunkoczi, G.; Chen, V. B.; Davis, I. W.; Echols, N.; Headd, J. J.; Hung, L. W.; Kapral, G. J.; Grosse-Kunstleve, R. W.; McCoy, A. J.; Moriarty, N. W.; Oeffner, R.; Read, R. J.; Richardson, D. C.; Richardson, J. S.; Terwilliger, T. C.; Zwart, P. H. PHENIX: a comprehensive Python-based system for macromolecular structure solution. *Acta Crystallogr., Sect. D: Biol. Crystallogr.* **2010**, *66*, 213–221.
(53) Emsley, P.; Cowtan, K. Coot: model-building tools for molecular graphics. *Acta Crystallogr., Sect. D: Biol. Crystallogr.* **2004**, *60*, 2126–2132.
(54) Schuttelkopf, A. W.; van Aalten, D. M. F. PRODRG: a tool for high-throughput crystallography of protein−ligand complexes. *Acta Crystallogr., Sect. D: Biol. Crystallogr.* **2004**, *60*, 1355–1363.